EXPERIMENTAL BEHAVIOUR OF RC BEAMS SHEAR STRENGTHENED WITH NSM CFRP LAMINATES

S. J. E. Dias[1] and J. A. O. Barros[2]

[1] Auxiliary Prof., ISISE, Dep. of Civil Eng., Univ. of Minho, Azurém, 4810-058 Guimarães, Portugal

[2] Associate Prof., ISISE, Dep. of Civil Eng., Univ. of Minho, Azurém, 4810-058 Guimarães, Portugal

Abstract

The Near Surface Mounted (NSM) is one of the most recent techniques applied for the increase of the shear resistance of Reinforced Concrete (RC) beams. This technique involves the installation of Carbon Fiber Reinforcement Polymers (CFRP) laminates into thin slits open on the concrete cover of the elements to strengthen. The effectiveness of this technique for the shear strengthening of T cross section RC beams was assessed by experimental research. For this purpose, three inclinations of laminates were tested (45º, 60º and 90º) and, for each inclination, three percentages of CFRP were applied in RC beams with a percentage of steel stirrups of 0.10% (ρ_{sw}). The highest percentage of laminates was designed to provide a maximum load similar to the reference RC beam, which was reinforced with a reinforcement ratio of steel stirrups of 0.28% (ρ_{sw} = 0.28%). For each percentage of laminates, a homologous RC beam strengthened with unidirectional U-shaped CFRP wet lay-up sheets (discrete strips) applied according to the Externally Bonded Reinforcement (EBR) technique was also tested, with the purpose of comparing the effectiveness of these two CFRP strengthening techniques. To evaluate the influence of the percentage of steel stirrups in the effectiveness of the NSM technique, some of the abovementioned CFRP configurations were also applied in beams with ρ_{sw} = 0.17%.

KEYWORDS: CFRP laminates, Experimental behaviour, NSM, RC beams, Shear strengthening

1. Introduction

The performance of a technique for the strengthening of Reinforced Concrete (RC) structures is dependent on several factors, such as: costs of the applied materials and human resources mobilized; period of time to execute the

[1] Author to whom the correspondence should be sent (sdias@civil.uminho.pt).

strengthening operations; period of inactivity that is eventually necessary for the execution of the strengthening process. The long term performance assured by the strengthening technique, and the level of interference it introduces in terms of architectural and aesthetic point-of-views are also relevant aspects for the evaluation of the effectiveness of the strengthening technique. In this context, it is now generally accepted that the strengthening techniques based on the use of Carbon Fiber Reinforcement Polymers (CFRP) composites materials provide solutions that compete with the traditional strengthening techniques applied in RC structures.

To increase the shear resistance of RC beams, CFRP (sheets or laminates) can be applied on the faces of the elements to be strengthened, using the Externally Bonded Reinforcing (EBR) technique (the fibers are positioned orthogonally to the beam's axis, or as orthogonal as possible to the predicted direction of the shear failure crack, or to the already existing shear cracks). Adopting the EBR technique, several researchers have verified that the shear resistance of RC beams can be significantly increased [1]. However, due to the premature debonding of the CFRP systems, the maximum strain that can be applied in these systems is well below of their ultimate strain. To increase the effectiveness of the CFRP for the shear strengthening of RC beams, the Near Surface Mounted (NSM) technique was proposed. The NSM involves the installation of narrow strips of CFRP laminates, of rectangular cross section, into thin slits open on the concrete cover of the lateral faces of the beams [2].

Experimental research has demonstrated that the NSM provides higher strengthening effectiveness than the EBR technique. This fact is derived from the larger CFRP laminate-concrete bond stress that can be mobilized in the NSM technique (both faces of the CFRP are bonded to concrete) [3-5]. A further advantage of the NSM is its ability to significantly reduce the probability of harm resulting from acts of vandalism, mechanical damages and aging effects. When NSM is used, the appearance of a structural element is practically unaffected by the strengthening intervention.

This work presents the results of the experimental program carried out to evaluate the influence of the percentage and orientation of CFRP in the behaviour of reinforced concrete T-beams, shear strengthened according to the NSM technique. The performance of this technique is evaluated by comparing the behaviour of the beams strengthened by the NSM technique with the behaviour of: i) the unstrengthened reference beam; ii) the homologous RC beams strengthened with U-shape CFRP wet lay-up sheets (discrete strips) applied according to the EBR technique; iii) the homologous RC beam with an additional amount of vertical steel stirrups (beam with ρ_{sw} = 0.28%). Furthermore, the influence of the percentage of existing steel stirrups in the performance of the NSM technique is also analysed. The experimental program is outlined, and the specimens, materials and test set-up are described. The results are

presented and analyzed in terms of the structural behavior of the tested beams, modes of failure and effectiveness of the CFRP shear strengthening configurations.

2. Experimental program

2.1 Beam prototypes

Fig. 1 presents the T cross section of the beams adopted in the experimental program, the lateral geometry of the type of beam and the steel reinforcement common to all tested beams. The reinforcement systems were designed to assure the occurrence of shear failure mode for all the tested beams. To localize the shear failure in only one of the beam shear spans, a three point loading configuration with a distinct length for the beam shear spans was selected, as shown in Fig. 1. The monitored beam span (L_i) is 2.5 times the effective depth of the beam ($L_i/d=2.5$), since, according to the available research [6], this is the minimum value that assures a negligible arch effect. To avoid shear failure in the L_r beam span, steel stirrups with 6 mm of diameter at a spacing of 75 mm (ϕ6@75mm) were applied in this span. The differences between the tested beams are restricted to the shear reinforcement systems applied in the L_i beam span.

The experimental program is composed of four reference beams and two groups of CFRP shear-strengthened beams. The reference beams (Fig. 2) consists of: one beam without any shear reinforcement (C-R beam); one beam with steel stirrups ϕ6@300mm (2S-R beam, with a percentage of stirrups, ρ_{sw}, of 0.10%); one beam with steel stirrups ϕ6@180mm (4S-R beam, with ρ_{sw} = 0.17%); one beam with steel stirrups ϕ6@112.5mm (7S-R beam, with ρ_{sw} = 0.28%).

For the CFRP shear-strengthened beams, the first group is composed of twelve beams with the percentage of stirrups adopted in the 2S-R reference beam (ρ_{sw} = 0.10%) and having the CFRP shear strengthening arrangements indicated in Table 1 and Fig. 3. Nine of these beams are strengthened according to the NSM technique, where three distinct percentages of CFRP laminates are considered and, for each CFRP percentage, three inclinations for the laminates are analyzed: 90º, 60º and 45º. The other three beams were strengthened according to the EBR technique, applying strips of unidirectional CFRP wet lay-up sheets of U configuration. The CFRP shear strengthening percentage, ρ_{fw}, was obtained from:

$$\rho_{fw} = \frac{2 \cdot a_f \cdot b_f}{b_w \cdot s_f \cdot \sin\theta_f} \quad (1)$$

where, for NSM beams, a_f = 1.4 mm and b_f = 9.5 mm are the dimensions of the laminate cross section. In equation (1), b_w = 180 mm is the width of the beam's web, and s_f and θ_f represent the spacing and the inclination of the CFRP, respectively. In the case of beams strengthened according to the EBR technique, a_f = 0.176 mm and b_f = 60 mm are the thickness and the width of the wet lay-up strips of CFRP sheet (if the number of layers, n, is greater than 1, $a_f = 0.176 \times n$).

The highest percentage of laminates of distinct orientations applied in beams with ρ_{sw} = 0.10% was evaluated to assure that the corresponding beams (2S-10LV, 2S-10LI45 and 2S-9LI60: see Table 1 and Fig. 3) had a maximum load similar to the beam reinforced with the highest value of ρ_{sw} (ϕ6@112.5mm, the 7S-R beam). For this purpose, it was assumed that a CFRP laminate works like a steel stirrup, however, instead of considering the yield stress of the material, a stress in the laminates corresponding to a strain of 0.5% was adopted since this is a compromise between the maximum value recommended by ACI [7] for the EBR (0.4%), and the 0.59% value obtained in pullout bending tests with NSM strengthening technique using CFRP laminates [8]. For the lowest (beams 2S-4LV, 2S-4LI45 and 2S-4LI60: see Fig. 3) and intermediate (beams 2S-7LV, 2S-7LI45 and 2S-6LI60: see Fig. 3) percentage of laminates the spacing of laminates for each θ_f (90º, 60º and 45º) was obtained with the purpose that the contribution of the CFRP would be similar in these beams. For the EBR strengthened beams, by applying the formulation recommended by the ACI [7], the percentages of discrete strips of wet lay-up CFRP sheet were evaluated in order to assure a load carrying capacity similar to the corresponding NSM strengthened series of beams (see Table 1 and Fig. 3).

The second group of CFRP shear-strengthened beams (see Table 1 and Fig. 4) is comprised by six beams that have the percentage of stirrups used in the 4S-R reference beam (ρ_{sw} = 0.17%), and the adopted NSM strengthening configurations were those corresponding to the intermediate and the lowest percentage of laminates applied in the first group of beams. The two groups of the beams with CFRP were prepared in order to be also possible the study of the influence of the amount of existing steel stirrups on the effectiveness of the NSM shear strengthening technique.

The laminates and the strips of sheet were distributed along the AB line represented in Fig. 1, where A represents the beam's support at its "test side" and B is obtained by assuming load degradation at 45º.

The three point beam bending tests (Fig. 1) were carried out using a servo closed-loop control equipment, taking the signal read in the displacement transducer (LVDT) placed at the loaded section, in order to control the test at a deflection rate of 0.01 mm/second. To avoid concrete spalling at the most loaded beam's support, a confinement

system based on the use of wet lay-up CFRP sheets (three layers with the fibers direction coinciding with the beam axis direction) was applied according to the configuration illustrated in Fig. 1.

With the purpose of obtaining the strain variation along one (beams with $\rho_{sw} = 0.17\%$) or two (beams with $\rho_{sw} = 0.10\%$) laminates and two strips of sheet that have the highest probability of providing the largest contribution for the shear strengthening of the RC beam, four strain gauges (SG_L on laminates and SG_M on the sheets) were bonded in each CFRP according to the arrangement represented in Fig. 5. Adopting the same principle, one steel stirrup was monitored with three strain gauges (SG_S) installed according to the configuration represented in Fig. 5. The location of the monitored laminates, strips of sheet and stirrups in the tested beams is represented in Fig. 3 (beams with $\rho_{sw} = 0.10\%$) and Fig. 4 (beams with $\rho_{sw} = 0.17\%$).

2.2 Material properties

The concrete compressive strength was evaluated at 28 days and at the age of the beam tests, carrying out direct compression tests with cylinders of 150 mm diameter and 300 mm height, according to EN 206-1 [9]. In the tested beams, high bond steel bars of 6, 12, 16 and 32 mm diameter were used. The values of their main tensile properties were obtained from uniaxial tensile tests performed according to the recommendations of EN 10002-1 [10].

The tensile properties of the CFK 150/2000 S&P laminates were characterized by uniaxial tensile tests carried out according to ISO 527-5 [11]. Electrical strain gauges and optical fiber sensors were used to measure the CFRP strains during the test (Fig. 6a), both positioned in the central zone of the laminate (one on each side of the CFRP). Fig. 6b shows the typical stress *vs* strain diagram obtained in uniaxial tensile tests with CFRP laminates, where it is possible to see that the results obtained with the two types of sensors were very similar. The typical failure mode of the laminates is represented in Fig. 6c. Table 2 includes the average values obtained from these experimental programs.

The tensile properties of the wet lay-up CFRP sheet, S&P C240 - 300g/m^2, were characterized elsewhere [12] and are summarized in Table 2. The MBrace Resin 220 [13] epoxy adhesive was used to bond the laminates to the concrete, while MBrace Resin 50 [13] primer and MBrace Resin 55 [13] epoxy resin were used in the application of the wet lay-up strips of CFRP sheets.

To evaluate the bond conditions between the CFRP EBR system and the concrete substrate, pull-off tests were carried out. This type of tests consists of the evaluation of the tensile load to pull one steel plate with a diameter equal to 45 mm that is bonded to the CFRP (Fig. 7a and Fig. 7b). To restrict the applied load to a well defined area, a partial core was executed (bond surface and steel plate have the same area). The bond strength value, $f_{ct,p}$, is

obtained dividing the maximum tensile load by the area of the steel plate. The steel plates were bonded to CFRP strips of the EBR shear strengthened beams (Fig. 7a). The average values of bond strength ($f_{ctm,p}$) were 3.5 MPa (three plates), 3.2 MPa (four plates) and 3.1 MPa (four plates) for the plates of the 2S-4M, 2S-7M(1) and 2S-7M(2) beams, respectively. The average value of these bond strengths was 3.3 MPa, which is higher than the limit (1.4 MPa) recommended by the ACI [7] for the strengthening of RC members with externally bonded FRP reinforcement. In the pull-off tests the failure occurred in the concrete, having the steel plates a thin layer of concrete, which indicates that concrete fracture was the governing failure mode (Fig. 7c).

2.3 Strengthening technique

To apply the precured CFRP laminates using the NSM technique, the following procedures were executed: 1) using a diamond cutter, slits of 4-5 mm width and 12-15 mm depth were opened on the concrete cover (of about 22 mm thickness) of the lateral faces of the beam's web, according to the pre-defined arrangement for the laminates (the laminates were not anchored into the beam's flange; they were restricted to the beam's web); 2) the slits were cleaned by compressed air; 3) the laminate, supplied in rolls of 150 m, and with the cross section of 1.4x9.5 mm^2, were cut with the desirable length and cleaned with acetone; 4) the epoxy adhesive was produced according to the supplier recommendations; 5) the slits were filled with the adhesive; 6) a layer of adhesive was applied on the faces of the laminates; and 7) the laminates were inserted into the slits and adhesive in excess was removed.

To apply the wet lay-up CFRP strengthening system using the EBR technique, the following procedures were done: 1) on the zones of the beam's surfaces where the strips of CFRP sheet were planned to be glued, an emery was applied to remove the superficial cement paste and to round out the beam's edges (with a radius of about 20 mm); 2) the residues were removed by compressed air; 3) a layer of primer was applied to regularize the concrete surface and to enhance the adherence capacity of the CFRP to the concrete substrate; 4) the CFRP sheets were measured and cut in the desired shape and dimensions; and 5) U-shaped CFRP strips, composed of one (2S-4M and 2S-7M(1) beams) or two layers (2S-7M(2) beam), were glued to the bottom and to the lateral faces of the beam, by epoxy resin. The primer and the epoxy resin were produced according to the supplier recommendations.

To guarantee a proper curing of the adhesive (NSM) and resin (EBR), at least one week passed between the beam strengthening operations and the beam test.

3. Results

3.1 Beams with ρ_{sw} = 0.10%

3.1.1 Load carrying capacity of the tested beams

The relationship between the applied force and the deflection at the loaded section (u_{LS}) for the tested beams with ρ_{sw} = 0.10% and 7S-R beam is represented in the left part of Fig. 8. As Fig. 8b shows, ΔF represents the increase of the load provided by a shear strengthening system, while $F^{2S\text{-}R}$ is the load capacity of the 2S-R reference beam. For deflections greater than the corresponding to the formation of the first shear crack in the 2S-R reference beam, the $\Delta F/F^{2S\text{-}R}$ ratio was evaluated, and the $\Delta F/F^{2S\text{-}R}$ *vs* u_{LS} relationship is depicted in the right column of Fig. 8. The maximum value of the $\Delta F/F^{2S\text{-}R}$ ratio, $\left(\Delta F/F^{2S\text{-}R}\right)_{max}$, is herein designated by strengthening efficacy index. For the tested beams, the $\left(\Delta F/F^{2S\text{-}R}\right)_{max}$ value and the corresponding deflection, $u_{\left(\Delta F/F^{2S-R}\right)_{\max}}$, are indicated in Table 3. Assuming that $\Delta F_{max} = F_{max} - F_{max}^{2S\text{-}R}$, being $F_{max}^{2S\text{-}R}$ and F_{max} the load carrying capacity (maximum force) of the 2S-R reference beam and of the shear reinforced beam, respectively, the $\Delta F_{max}/F_{max}^{2S\text{-}R}$ ratio was evaluated and is included in Table 3. The load carrying capacity of the 7S-R reference beam ($F_{max}^{7S\text{-}R}$) was also determined, and the values of $F_{max}/F_{max}^{7S\text{-}R}$ ratio are indicated in Table 3.

The results included in Table 3 and represented in Fig. 8 show that, for deflections higher than the one corresponding to the formation of the first shear crack in the 2S-R reference beam (u_{LS} = 2.15 mm), apart 2S-7LV beam, the adopted CFRP configurations provided an increase in the beam's load carrying capacity. In fact, the decrease of stiffness observed in the 2S-R reference beam when the first shear crack was formed was not so significant in the CFRP shear strengthened beams. This reveals that the CFRP laminates bridging the surfaces of the shear crack offer resistance, mainly, to crack opening, resulting a smaller degradation of the shear stress transfer between the faces of the crack due to aggregate interlock effect. Therefore, for deflections above the deflection corresponding to the formation of the shear crack in the 2S-R reference beam, an increase of the beam's stiffness is observed in the shear strengthened beams. The crack opening resisting mechanisms provided by the laminates bridging the crack also contribute to increase the load at which stirrups enter in their plastic phase.

The strengthening arrangements with NSM CFRP laminates provided an increase in terms of the maximum load ($\Delta F_{max}/F_{max}^{2S\text{-}R}$) that has ranged between 11.1% and 47.0%. Apart 2S-4LV beam, it was verified that $\Delta F_{max}/F_{max}^{2S\text{-}R} = \left(\Delta F/F^{2S\text{-}R}\right)_{max}$. From the results obtained in NSM and EBR beams, the following considerations

can be pointed out: i) using the load carrying capacity F_{max} of the 2S-R beam (reference beam) for comparison purposes, the beams strengthened by NSM and EBR solutions provided an average increase of 30.3% and 10.4%, respectively; ii) the average value of F_{max} for the beams with the highest percentage of laminates (2S-10LV, 2S-10LI45 and 2S-9LI60 beams) was 90% of $F_{max}^{7S\text{-}R}$. The maximum load of the 2S-7M(2) EBR beam, however, was only 79% of the $F_{max}^{7S\text{-}R}$; iii) The average value of $\left(\Delta F / F^{2S\text{-}R}\right)_{max}$ for the NSM beams and EBR beams was 30.9% and 18.1%, respectively; iv) in general the NSM strengthened beams were stiffer than the EBR strengthened beams, which reflects the better performance of the NSM laminates in terms of controlling the shear cracks. These considerations indicate that NSM strengthened beams had better structural behavior than EBR strengthened beams.

3.1.2 Failure modes

As was expected, all the tested beams failed in shear in the L_i beam span (Fig. 9). In this figure, the steel stirrups in the smaller beam shear span are indicated by vertical lines, and the circles indicate the zone where stirrups have ruptured.

When the maximum load of the C-R beam was attained the shear failure crack widened abruptly. The maximum load of the 2S-R and 7S-R beams was attained when one stirrup crossing the shear failure crack has ruptured.

In general, in the NSM beams strengthened with the minimum ρ_{fw}, the laminates failed by "debonding". However, in the present context "debonding" should not be assumed as a pure debonding failure mode of the laminate, since along its bond length, parts of concrete were adhered to the laminate, indicating that failure includes debond and concrete fracture (see the detail of the 2S-4LI45 beam). In the NSM beams strengthened with the intermediate ρ_{fw}, and mainly in beams with the largest ρ_{fw}, the separation of parts of the concrete cover was the typical failure mode, which had already been observed in previous experimental programs [14-16]. The tendency for the occurrence of the detachment of the concrete cover with the decrease of the spacing between laminates, which reflects a detrimental effect of the mutual interference between consecutive laminates (group effect – see the detail of the 2S-7LI45 and 2S-10LI45), was recently captured by the innovative analytical model developed by Bianco *et al.* [17] for the prediction of the contribution of the NSM laminates for the shear resistance of RC beams.

In the EBR beams (2S-4M, 2S-7M(1) and 2S-7M(2)) the failure mode was independent of the CFRP percentage and consisted of the debond of the wet lay-up CFRP sheets from the concrete (see Fig. 9). The maximum load of the 2S-4M beam was attained just before the first strip of sheet has debonded. In the case of 2S-7M(1) and 2S-7M(2)

beams the maximum load occurred just after two strips of sheet have debonded. The effect of this occurrence can be observed in the relationship between force and deflection at the loaded section of the beams (Fig. 8b and 8c).

3.1.3 Effect of the percentage and inclination of the CFRP

Fig. 10 represents the relationship between the strengthening efficacy, $\Delta F_{max} / F_{max}^{2S\text{-}R}$, provided by the CFRP arrangements, and the CFRP percentage (ρ_{fw}) for the analyzed NSM and EBR shear strengthening configurations (see Tables 1 and 3). This figure shows that, regardless the ρ_{fw}, the arrangement of laminates at 45º was the most effective among the adopted CFRP shear strengthening configurations, and the EBR was not so effective as NSM technique. It is also observed that inclined laminates were more effective than vertical laminates. This is justified by the orientation of the shear failure cracks that had a tendency to be almost orthogonal to the inclined laminates. Furthermore, for vertical laminates the total resisting bond length of the CFRP is lower than for inclined laminates. The NSM beams with the lowest percentage of inclined laminates had better performance than the EBR beam with the highest percentage of CFRP. Fig. 10 also shows that, independently of the orientation of the laminates, and for the range of ρ_{fw} values considered in the present experimental program, $\Delta F_{max} / F_{max}^{2S\text{-}R}$ has increased, almost linearly, with the increase of ρ_{fw}. This tendency was verified in both NSM and EBR shear strengthening techniques.

3.1.4 Strains in the CFRP and steel stirrups

Fig. 11 represents the relationship between ε_{CFRP}^{max} and ρ_{fw} (continuous line) and between $(\varepsilon_{CFRP}^{max})_{med}$ and ρ_{fw} (dashed line), where ε_{CFRP}^{max} is the maximum strain recorded up to the maximum load of the beams in the strain gauges installed in the monitored laminates and sheets (see Fig. 3 and Fig. 5), and $(\varepsilon_{CFRP}^{max})_{med}$ is the average value of the maximum strains registered in each monitored CFRP (two per beam). It can be verified that ε_{CFRP}^{max} in the laminates ranged from 0.56% in the 2S-4LV beam and 1.08% in the 2S-4LI45 (see Table 3). In terms of $(\varepsilon_{CFRP}^{max})_{med}$, the variation was between 0.55% in the 2S-4LV and 1.03% in the 2S-4LI45 (see Table 3). Fig. 11 shows that the maximum values for the ε_{CFRP}^{max} and $(\varepsilon_{CFRP}^{max})_{med}$ were recorded in the NSM beams, while the minimum values were registered in the EBR beams. This fact indicates that the NSM technique mobilizes more effectively the tensile properties of the CFRP (the average value of ε_{CFRP}^{max} for NSM and EBR beams was 0.84% and 0.65%, respectively).

In terms of CFRP orientation, the average value of the maximum strain (ε_{CFRP}^{max}) was 0.88%, 0.94% and 0.70% for the beams with laminates at 45º, 60º and 90º, respectively. These values ranged from 44% to 59% of the CFRP ultimate strain (ε_{fu} = 1.6% - see Table 2).

Apart the beams with vertical laminates, both ε_{CFRP}^{max} and $(\varepsilon_{CFRP}^{max})_{med}$ decreased with the increase of ρ_{fw}. This can be justified by the crack pattern and failure modes occurred. In fact, with the increase of ρ_{fw} the crack pattern was more diffuse and the concrete cover that includes the laminates had a tendency to separate from the concrete core of the beams, resulting more uniform strain distributions along the CFRP elements. In these cases, the probability of occurring high gradients of strains, typical of beams with low ρ_{fw}, is reduced.

A very important aspect of the effectiveness of the NSM technique, regarding the analyzed beams, is its capacity to mobilize the yield strain of the stirrups crossed by the diagonal shear failure crack.

3.2 Influence of the percentage of steel stirrups on the effectiveness of the NSM technique

The diagrams force versus deflection at loaded section (F-u_{LS}) in the tested beams with ρ_{sw} = 0.17% are represented in Fig. 12, where it is possible to see that the typical behavior of the strengthened beams is similar to the NSM beams with ρ_{sw} = 0.10%. The CFRP laminates provided an increase of the beam's stiffness, maximum load (F_{max}) and deflection at F_{max} (u_{Fmax}) - see Table 4. Regardless the percentage of CFRP, the inclined laminates were more effective than vertical laminates. The increase of the percentage of CFRP conducted to an increase of the shear resistance of the strengthened beams. The failure modes of the NSM beams with ρ_{sw} = 0.17% (see Fig. 13) were similar to those observed in NSM beams with ρ_{sw} = 0.10%.

To evaluate the influence of the percentage of steel stirrups on the effectiveness of the NSM technique, six arrangements of CFRP laminates were applied in beams with ρ_{sw} = 0.10% and in beams with ρ_{sw} = 0.17% (see Table 1). For these beams, the values of the $\Delta F_{max} / F_{max}^{ref}$ ratio and the maximum strain recorded in the laminates (ε_{CFRP}^{max}) for the NSM beams with ρ_{sw} = 0.10% ($F_{max}^{ref} = F_{max}^{2S\text{-}R}$) and ρ_{sw} = 0.17% ($F_{max}^{ref} = F_{max}^{4S\text{-}R}$) are included in Table 5. The $\Delta F_{max} / F_{max}^{ref}$ ratio is also represented in Fig. 14. According to the values into Table 5 and Fig. 14, the average value of the $\Delta F_{max} / F_{max}^{ref}$ ratio for NSM arrangements adopted in the beams with lower and higher percentage of steel stirrups was 29.6% and 21.1%, respectively (the values corresponding to the shear strengthening configuration with the lowest percentage of vertical laminates were excluded for this analysis). The better performance of the CFRP when applied

in the beams with ρ_{sw} = 0.10% was also observed in terms the $\Delta F/F^{ref}$ *vs* u_{LS} relationship (Fig. 15). Furthermore, in the group of beams of ρ_{sw} = 0.10%, larger maximum strain values were registered in the CFRP. The average value of the maximum strain recorded in the laminates up to the maximum load of the beams (ε_{CFRP}^{max}) was 0.87% for beams with ρ_{sw} = 0.10% and 0.83% for beams with ρ_{sw} = 0.17%.

The obtained experimental results show that the amount of existing steel stirrups plays a very important role on the effectiveness of the NSM shear strengthening technique. In fact, this effectiveness was higher in the beams with the lower percentage of steel stirrups analysed (ρ_{sw} = 0.10%). According to Fig. 14, for an increase from 0.1% to 0.17% in the percentage of steel stirrups in the L_i beam span (about 70%), the NSM shear strengthening effectiveness decreased in about 70% (the values corresponding to the lower percentage of vertical laminates were excluded for this evaluation). It emerges that a formulation for the prediction of the NSM shear strengthening contribution cannot neglect the percentage of existing steel stirrups.

4. Conclusions

The effectiveness of the EBR and NSM techniques for the shear strengthening of T cross section RC beams that also include a certain percentage of steel stirrups was compared by carrying out an experimental program. The effectiveness of the distinct CFRP shear strengthening arrangements was appraised by assessing their contribution in terms of load carrying capacity, stiffness of the response of the beams after the formation of the shear failure crack in the reference beam, maximum strains measured in the CFRP systems, and failure modes. In terms of the effectiveness of the NSM technique, the influence of the percentage and inclination of the laminates, and the influence of the percentage of existing steel stirrups was also evaluated.

From the obtained results it can be concluded that NSM technique was more effective than EBR, since NSM provided a higher increase, not only in terms of beam's load carrying capacity, represented by the $\Delta F_{max}/F_{max}^{2S\text{-}R}$ ratio, but also in terms of stiffness after shear crack formation, represented by the $\left(\Delta F/F^{2S\text{-}R}\right)_{max}$ ratio. The values of $\Delta F_{max}/F_{max}^{2S\text{-}R}$ and $\left(\Delta F/F^{2S\text{-}R}\right)_{max}$ of the EBR beams were 34% and 59% of the values obtained in the NSM beams. NSM also provided higher values of maximum strains measured in the CFRP.

When compared to the homologous conventionally shear reinforced beam (7S-R beam), the NSM shear strengthened beams (designed to have the same load carrying capacity of the 7S-R beam) presented 90% of the maximum load of the 7S-R beam, and higher stiffness, mainly after shear crack initiation, while EBR shear

strengthened beam had a maximum load that was 79% of the maximum load of the 7S-R beam, and similar stiffness up to the initiation of the debonding process of the wet lay-up CFRP strips of sheet.

Regardless of the percentage of CFRP and the percentage of existing steel stirrups, the inclined laminates were more effective than vertical laminates. An increase of the percentage of CFRP led to an increase of the beam's shear resistance. The contribution of the NSM CFRP laminates for the beam shear resistance was limited by the concrete tensile strength, since at failure, a certain concrete volume was attached to the laminates. An interaction between the percentage of steel stirrups and the CFRP laminates was observed, resulting a detrimental effect in terms of the effectiveness of the NSM technique for the shear resistance of RC beams.

An analytical formulation for the prediction of the NSM shear strengthening contribution should take into account the concrete mechanical properties, the percentage and orientation of the CFRP and the percentage of the existing steel stirrups.

ACKNOWLEDGEMENTS

The authors wish to acknowledge the support provided by the "Empreiteiros Casais", Degussa, S&P® and Secil (Unibetão, Braga). The study reported in this paper forms a part of the research program supported by FCT, PTDC/ECM/73099/2006.

REFERENCES

[1] Bousselham A. and Chaallal O., "Shear strengthening reinforced concrete beams with fiber-reinforced polymer: assessment of influencing parameters and required research", *ACI Structural Journal*, 101(2), 219-227 (2004).

[2] Barros, J.A.O. and Dias, S.J.E., "Shear strengthening of reinforced concrete beams with laminate strips of CFRP", Proceedings of the International Conference Composites in Constructions - CCC2003, Cosenza, Italy, 16-19 September, 289-294 (2003).

[3] Blaschko, M. and Zilch, K., "Rehabilitation of concrete structures with CFRP strips glued into slits", Proceedings of the Twelfth International Conference of Composite Materials, ICCM 12, Paris, France (1999).

[4] El-Hacha, R. and Riskalla, S.H., "Near-surface-mounted fiber-reinforced polymer reinforcements for flexural strengthening of concrete structures", *ACI Structural Journal*, 101(5), 717-726 (2004).

[5] Barros, J.A.O., Dias, S.J.E. and Lima, J.L.T., "Efficacy of CFRP-based techniques for the flexural and shear strengthening of concrete beams", *Journal Cement and Concrete Composites*, 29(3), 203-217 (2007).

[6] Collins, M. P., and Mitchell, D., "Prestresed Concrete Structures", Prentice-Hall, Inc., Englewood Cliffs, New Jersey (1997).

[7] ACI Committee 440, "Guide for the design and construction of externally bonded FRP systems for strengthening concrete structures", American Concrete Institute, 118 pp. (2002).

[8] Sena-Cruz, J.M. and Barros, J.A.O., "Bond between near-surface mounted CFRP laminate strips and concrete in structural strengthening", *Journal of Composites for Construction*, 8(6), 519-527 (2004).

[9] EN 206-1, "Concrete - Part 1: Specification, performance, production and conformity." European standard, CEN, 69 pp. (2000).

[10] EN 10002-1, "Metallic materials - Tensile testing. Part 1: Method of test (at ambient temperature)", European Standard, CEN, Brussels, Belgium, 35 pp. (1990).

[11] ISO 527-5, "Plastics - Determination of tensile properties - Part 5: Test conditions for unidirectional fibre-reinforced plastic composites", International Organization for Standardization (ISO), Geneva, Switzerland, 9 pp. (1997).

[12] Barros, J.A.O., Bonaldo, E. and Oliveira, J.T., *"Composite materials for the structural strengthening of reinforced masonry shells",* Proceedings of ACIC 07, Advanced Composites in Construction, 2-4 April, University of Bath, UK (2007).

[13] Degussa Construction Chemicals Portugal, Technical Report MBrace Resin 50, MBrace Resin 55 and MBrace Resin 220, May (2003).

[14] Barros, J.A.O. and Dias, S.J.E., "Near surface mounted CFRP laminates for shear strengthening of concrete beams", *Journal Cement and Concrete Composites*, 28(3), 276-292 (2006).

[15] Rizzo, A. and De Lorenzis, L., "Behaviour and capacity of RC beams strengthened in shear with NSM FRP reinforcement", *Construction and Building Materials*, 23, 1555-1567 (2009).

[16] Dias, S.J.E. and Barros, J.A.O., "Shear strengthening of T cross section reinforced concrete beams by near surface mounted technique", *Journal of Composites for Construction*, 12(3), 300-311 (2008).

[17] Bianco, V., Barros, J.A.O. and Monti, G., "Three dimensional mechanical model for simulating the NSM FRP strips shear strength contribution to RC beams", *Engineering Structures*, doi:10.1016/j.engstruct.2008.12.017 (2009).

TABLES AND FIGURES

List of Tables:

List of Figures:

Fig. 14 - Influence of the percentage of existing steel stirrups in the effectiveness of the NSM shear strengthening technique using CFRP laminates

Fig. 15 - $\Delta F/F^{ref}$ *vs* deflection at the loaded-section for the beams shear strengthened with NSM CFRP laminates (beams with ρ_{sw} = 0.10%: continuous line; beams with ρ_{sw} = 0.17%: dashed line): a) lowest percentage of CFRP; b) intermediate percentage of CFRP

Table 1 - CFRP shear reinforcement configurations of the tested beams

Beams		Shear strengthening	Quantity	Angle (º) [c]	CFRP spacing (mm)	CFRP percentage (%)
ρ_{sw} = 0.10% [a]	ρ_{sw} = 0.17% [b]					
2S-4LV	4S-4LV	NSM CFRP laminates	2×4 laminates (1.4×9.5 mm^2)	90	180	0.08
2S-7LV	4S-7LV		2×7 laminates (1.4×9.5 mm^2)	90	114	0.13
2S-10LV	-		2×10 laminates (1.4×9.5 mm^2)	90	80	0.18
2S-4LI45	4S-4LI45		2×4 laminates (1.4×9.5 mm^2)	45	275	0.08
2S-7LI45	4S-7LI45		2×7 laminates (1.4×9.5 mm^2)	45	157	0.13
2S-10LI45	-		2×10 laminates (1.4×9.5 mm^2)	45	110	0.19
2S-4LI60	4S-4LI60		2×4 laminates (1.4×9.5 mm^2)	60	243	0.07
2S-6LI60	4S-6LI60		2×6 laminates (1.4×9.5 mm^2)	60	162	0.11
2S-9LI60	-		2×9 laminates (1.4×9.5 mm^2)	60	108	0.16
2S-4M [d]	-	EBR CFRP wet lay-up sheets	4 strips of CFRP wet lay-up sheets U configuration - 1 layer (0.176×60 mm^2)	90	180	0.07
2S-7M(1) [e]	-		7 strips of CFRP wet lay-up sheets U configuration - 1 layer (0.176×60 mm^2)	90	114	0.10
2S-7M(2) [f]	-		7 strips of CFRP wet lay-up sheets U configuration - 2 layers (0.176×60 mm^2)	90	114	0.21

[a] 2S-R is the reference beam without CFRP (Fig. 2); [b] 4S-R is the reference beam without CFRP (Fig. 3); [c] Angle between the CFRP fiber direction and the beam axis; [d] The predicted load carrying capacity of this beam was similar to the 2S-4LV, 2S-4LI45 and 2S-4LI60 beams; [e] The predicted load carrying capacity of this beam was similar to the 2S-7LV, 2S-7LI45 and 2S-6LI60 beams; [f] The predicted load carrying capacity of this beam was similar to the 2S-10LV, 2S-10LI45 and 2S-9LI60 beams.

Table 2 - Values of the properties of intervening materials

Concrete	Compressive strength				
	f_{cm} = 31.7 MPa (at 28 days)			f_{cm} = 39.7 MPa (at 106 days - age of beam tests)	
Steel	Tensile strength	ϕ6	ϕ12	ϕ16	ϕ32
	f_{sym} (yield stress)	542 MPa	453 MPa	447 MPa	759 MPa
	f_{sum} (maximum stress)	594 MPa	591 MPa	566 MPa	902 MPa
CFRP Laminates	Maximum tensile strength	Young's Modulus		Maximum strain	
	f_{fum} = 2741.7 MPa	E_{fm} = 170.9 GPa		ε_{fu} = 1.60 %	
Wet lay-up CFRP sheet	Maximum tensile strength	Young's Modulus		Maximum strain	
	f_{fum} = 2862.9 MPa	E_{fm} = 218.4 GPa		ε_{fu} = 1.33 %	

Table 3 - Relevant results in terms of the load capacity up to beam's failure (ρ_{sw} = 0.10%)

Beams	$\left(\Delta F / F^{2S-R}\right)_{max}$ (%)	$u_{\left(\Delta F / F^{2S-R}\right)_{max}}$ [a] (mm)	F_{max} (kN)	$\Delta F_{max} / F_{max}^{2S-R}$ (%)	F_{max} / F_{max}^{7S-R}	ε_{CFRP}^{max} (%)	$(\varepsilon_{CFRP}^{max})_{med}$ (%)
C-R	-	-(7.48)	207.0	-	0.44	-	-
2S-R	0.0	- (5.88)	303.8	-	0.65	-	-
7S-R	53.9	8.78 (8.78)	467.5	53.9	1.00	-	-
2S-4LV	16.4	4.65 (7.14)	337.4	11.1	0.72	0.56	0.55
2S-7LV	23.1	7.17 (7.17)	374.1	23.1	0.80	0.77	0.71
2S-10LV	30.8	6.09 (6.09)	397.5	30.8	0.85	0.77	0.75
2S-4LI45	29.3	6.45 (6.45)	392.8	29.3	0.84	1.08	1.03
2S-7LI45	38.8	7.93 (7.93)	421.7	38.8	0.90	0.85	0.80
2S-10LI45	47.0	6.76 (6.76)	446.5	47.0	0.96	0.72	0.69
2S-4LI60	27.2	6.90 (6.90)	386.4	27.2	0.83	0.99	0.98
2S-6LI60	29.8	7.77 (7.87)	394.4	29.8	0.84	0.99	0.87
2S-9LI60	35.8	6.44 (6.44)	412.7	35.8	0.88	0.85	0.79
2S-4M	13.0	3.78 (4.79)	311.1	2.4	0.67	0.79	0.69
2S-7M(1)	19.4	4.32 (5.99)	325.1	7.0	0.70	0.68	0.57
2S-7M(2)	21.8	7.77 (7.77)	370.1	21.8	0.79	0.49	0.45

a The value into round brackets corresponds to the deflection at the loaded section when the maximum load occurred.

Table 4 - Relevant results in terms of the load capacity up to beam's failure (ρ_{sw} = 0.17%)

Beams	F_{max} (kN)	$\Delta F_{max} / F_{max}^{4S-R}$ (%)	$u_{F_{max}}$ (mm)
4S-R	371.4	-	6.25
4S-4LV	424.5	14.3	9.32
4S-7LV	427.4	15.1	9.75
4S-4LI45	442.5	19.1	7.93
4S-7LI45	478.1	28.7	8.26
4S-4LI60	443.8	19.5	6.91
4S-6LI60	457.6	23.2	7.31

Table 5 - Influence of the percentage of steel stirrups in the effectiveness of the NSM shear strengthening technique with CFRP laminates

CFRP		Beams (ρ_{sw} = 0.10%)	$\Delta F_{max} / F_{max}^{2S-R}$ (%)	ε_{CFRP}^{max} (%)	Beams (ρ_{sw} = 0.17%)	$\Delta F_{max} / F_{max}^{4S-R}$ (%)	ε_{CFRP}^{max} (%)
Percentage (%)	Angle (º)						
0.08	90	2S-4LV	11.1	0.56	4S-4LV	14.3	0.66
0.13	90	2S-7LV	23.1	0.77	4S-7LV	15.1	0.91
0.08	45	2S-4LI45	29.3	1.08	4S-4LI45	19.1	0.79
0.13	45	2S-7LI45	38.8	0.85	4S-7LI45	28.7	0.82
0.07	60	2S-4LI60	27.2	0.99	4S-4LI60	19.5	0.94
0.11	60	2S-6LI60	29.8	0.99	4S-6LI60	23.2	0.87

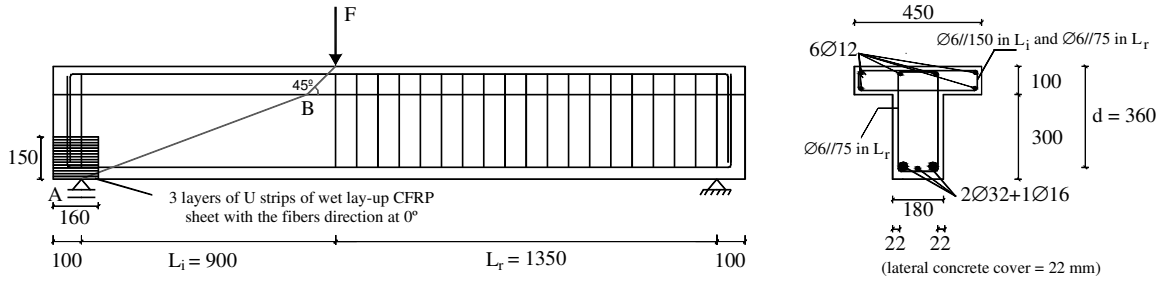

Fig. 1 - Geometry of the type of beam, steel reinforcements common to all beams, support and load conditions (dimensions in mm)

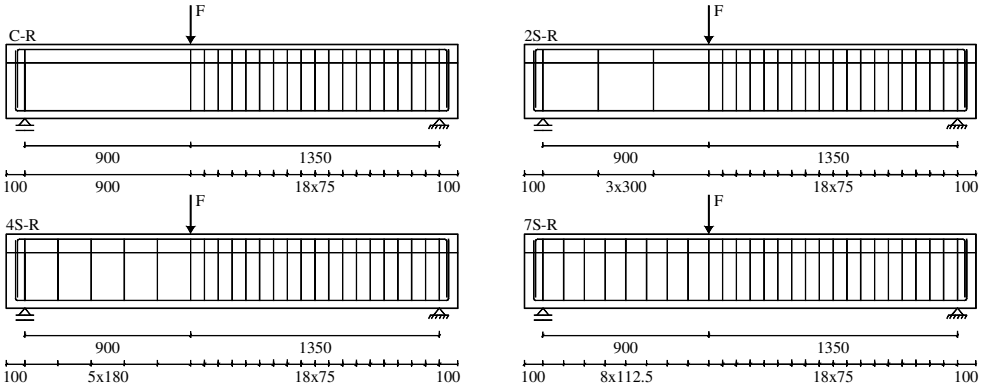

Fig. 2 - Details of the reference beams (dimensions in mm)

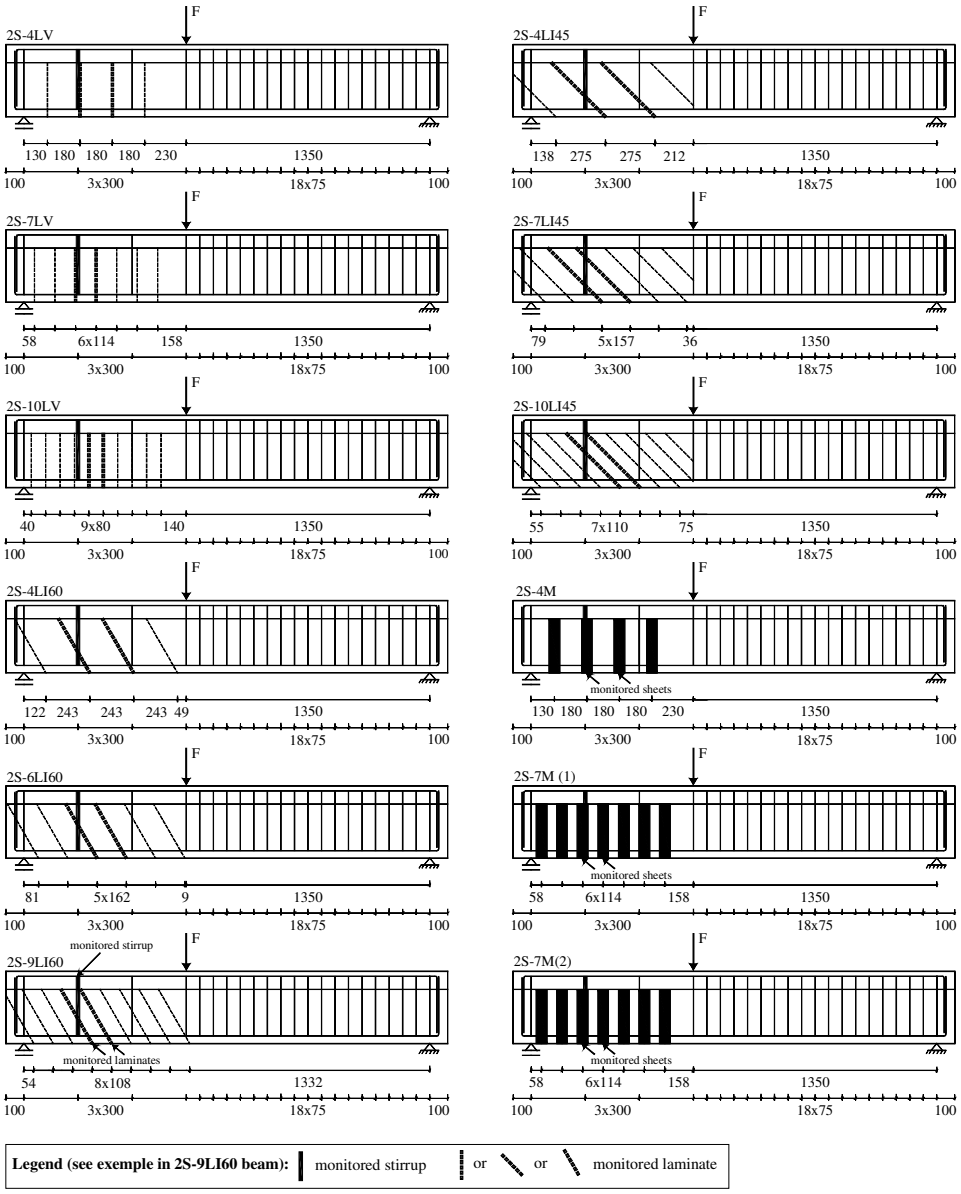

Fig. 3 - Localization of the steel stirrups (continuous line), laminates (dashed line) and strips of sheets in the CFRP shear strengthened beams with ρ_{sw} = 0.10% (dimensions in mm)

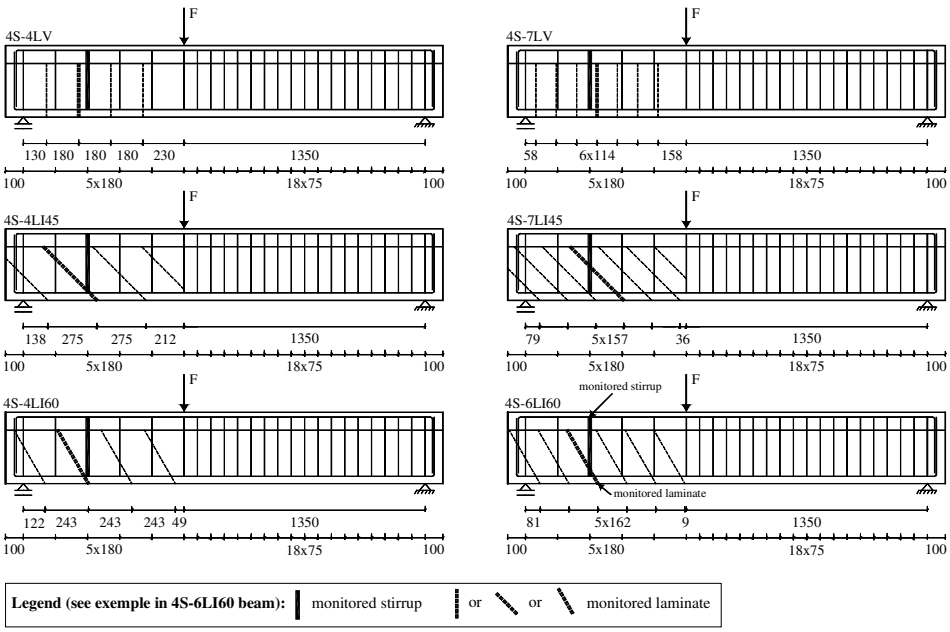

Fig. 4 - Localization of the steel stirrups (continuous line) and laminates (dashed line) in the CFRP shear strengthened beams with ρ_{sw} = 0.17% (dimensions in mm)

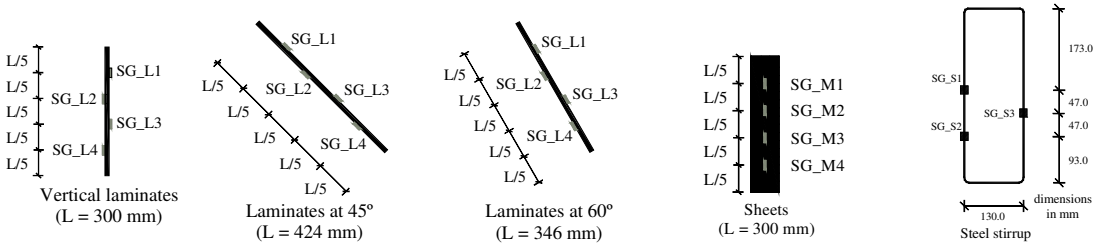

Fig. 5 - Positions of the strain gauges in the monitored laminates, strips of sheet and stirrups

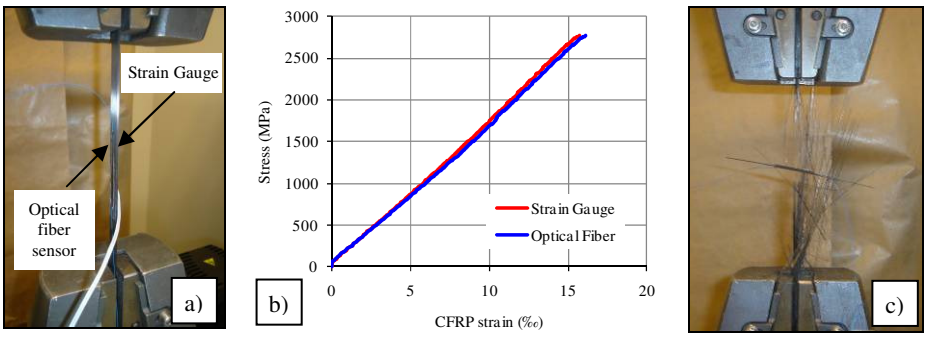

Fig. 6 - Experimental characterization of the CFRP laminates: a) test; b) stress *vs* CFRP strain relationship; c) typical failure mode

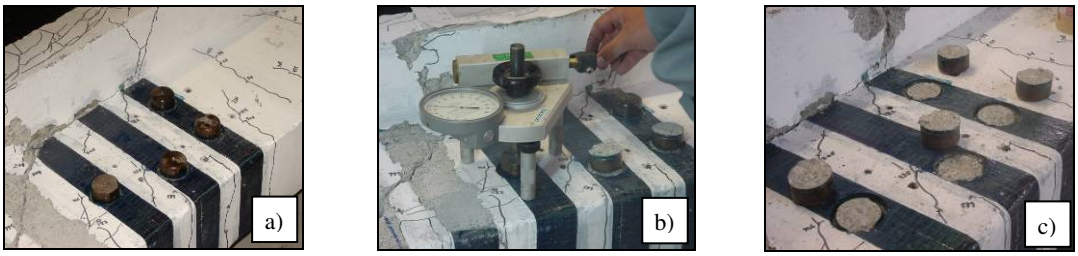

Fig. 7 - Pull-off tests: a) steel plates bonded to the CFRP; b) test; c) failure modes

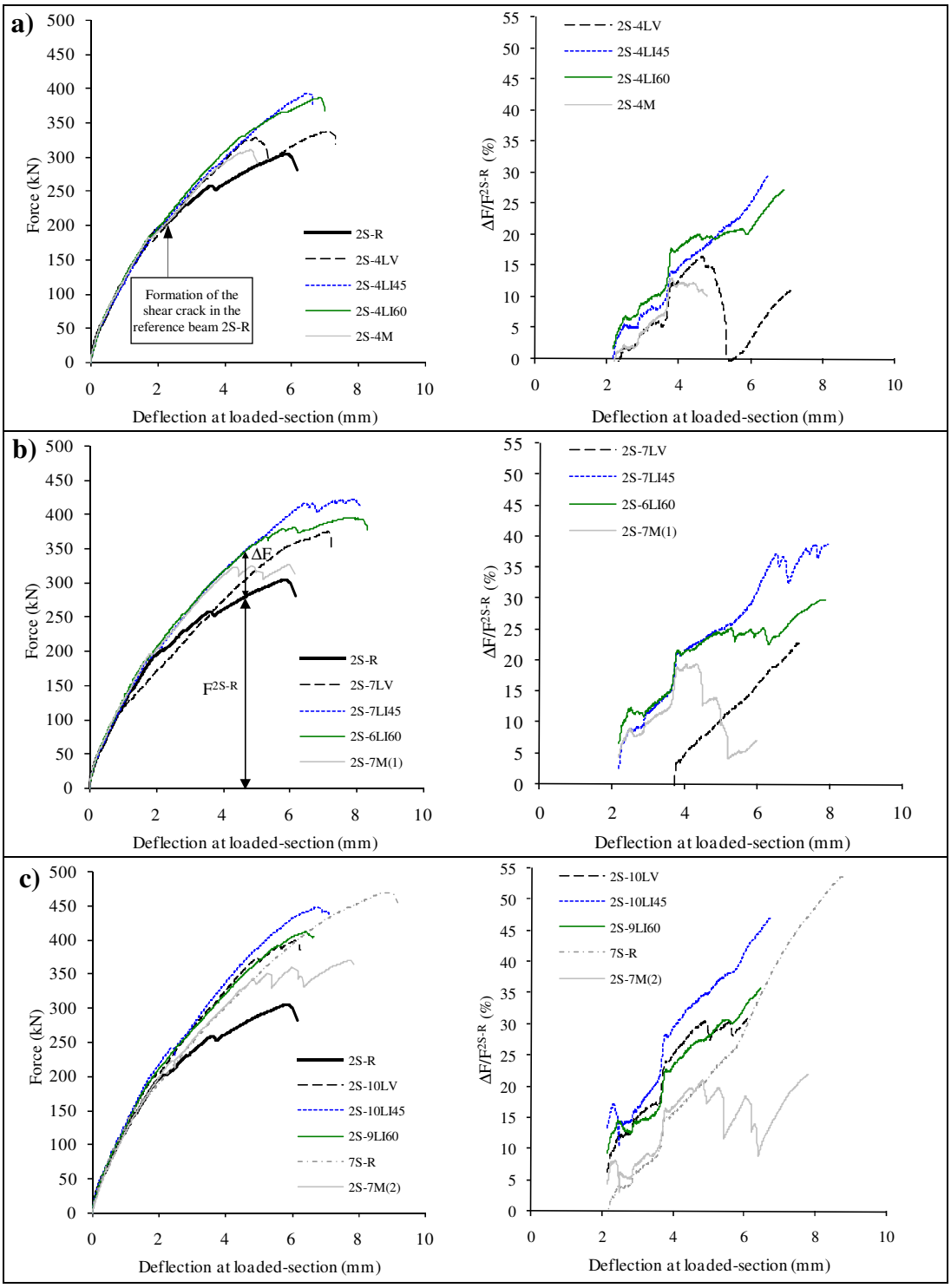

1 Fig. 8 - Force *vs* deflection at the loaded-section and $\Delta F/F^{2S-R}$ *vs* deflection at the loaded-section for the beams (ρ_{sw} =

2 0.10%) strengthened with the: a) lowest; b) intermediate; c) highest percentage of CFRP

3

4

5

6

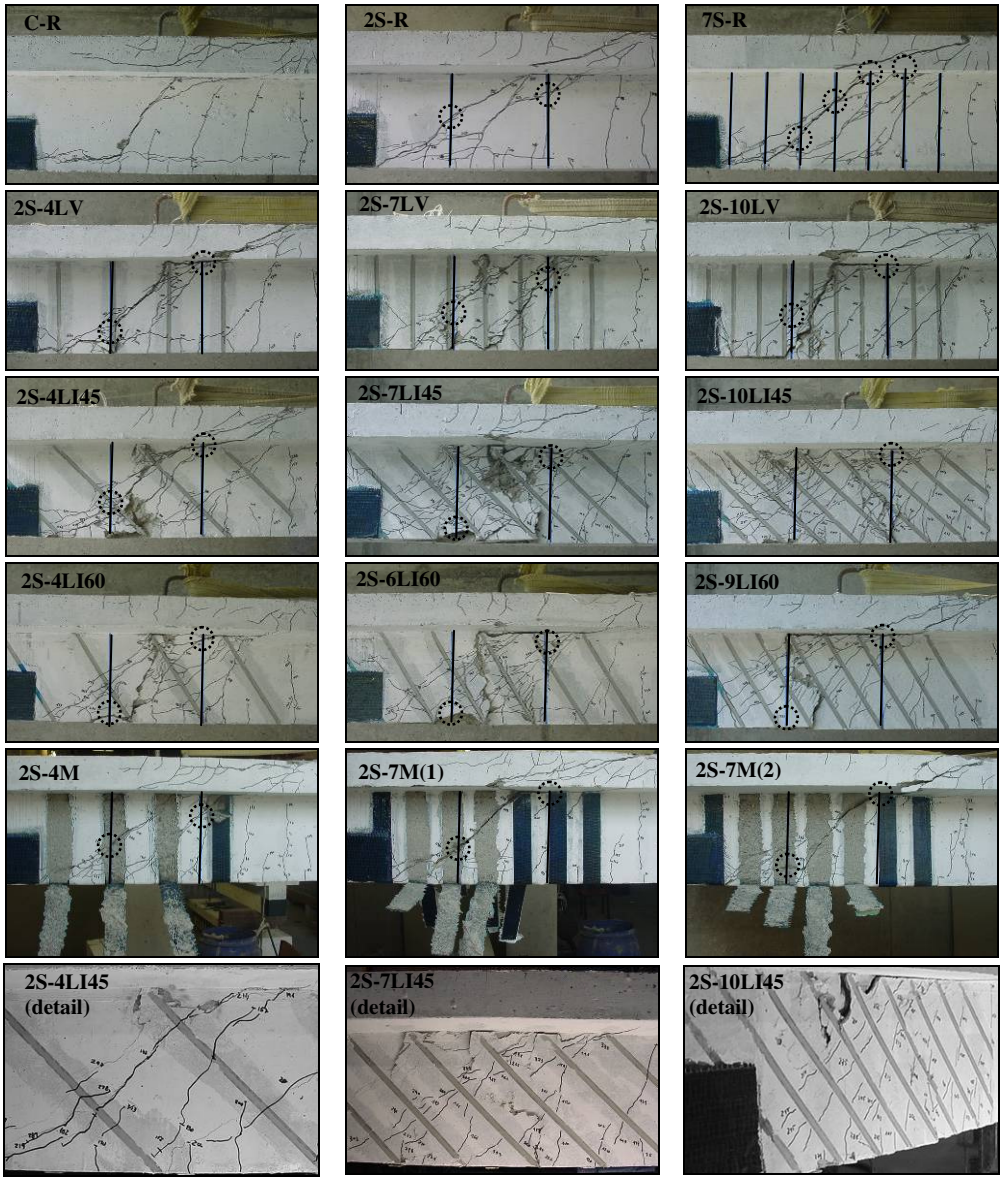

Fig. 9 - Details of the failure zones of the C-R and 7S-R beams, and strengthened beams with ρ_{sw} = 0.10%

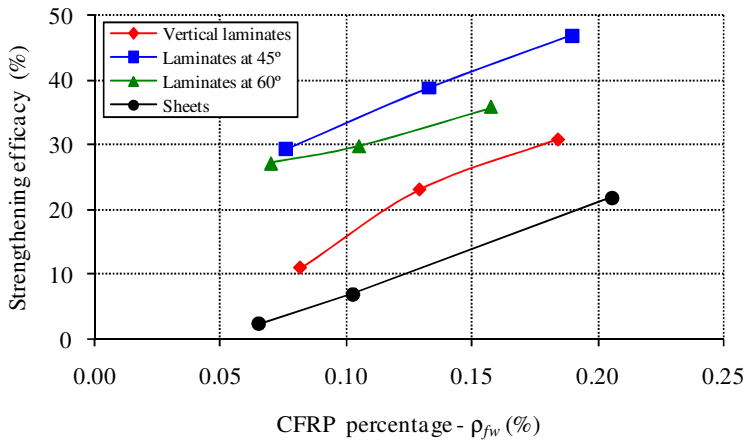

Fig. 10 - Strengthening efficacy ($\Delta F_{max} / F_{max}^{2S-R}$) *vs* CFRP percentage (ρ_{fw})

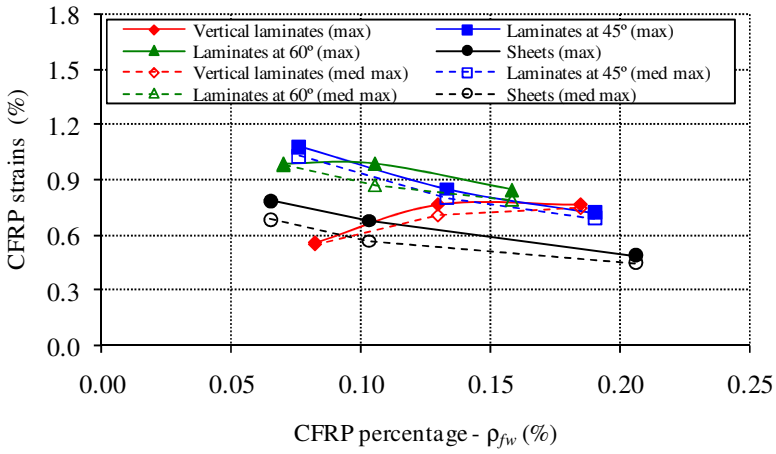

Fig. 11 - CFRP strains *vs* CFRP percentage (ρ_{fw})

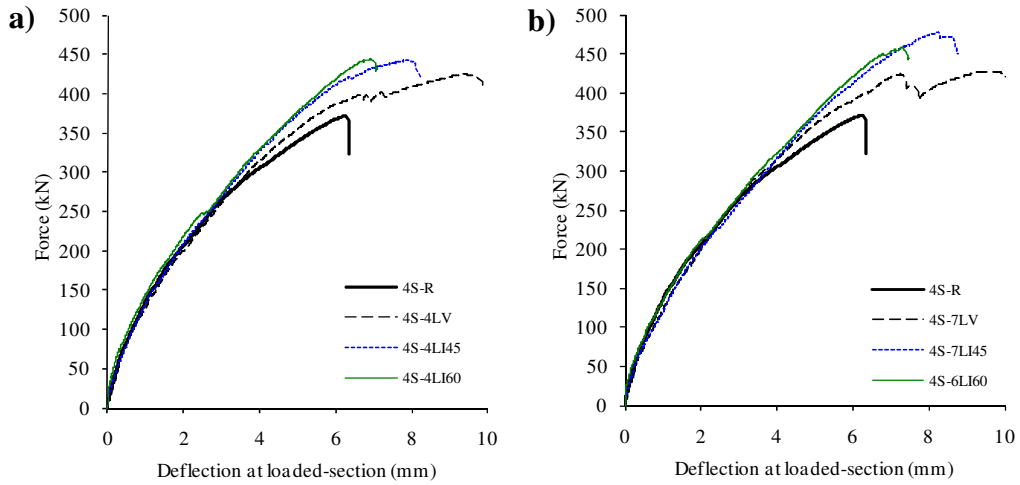

Fig. 12 - Force *vs* deflection for the beams with ρ_{sw} = 0.17%: a) lowest; b) intermediate percentage of CFRP

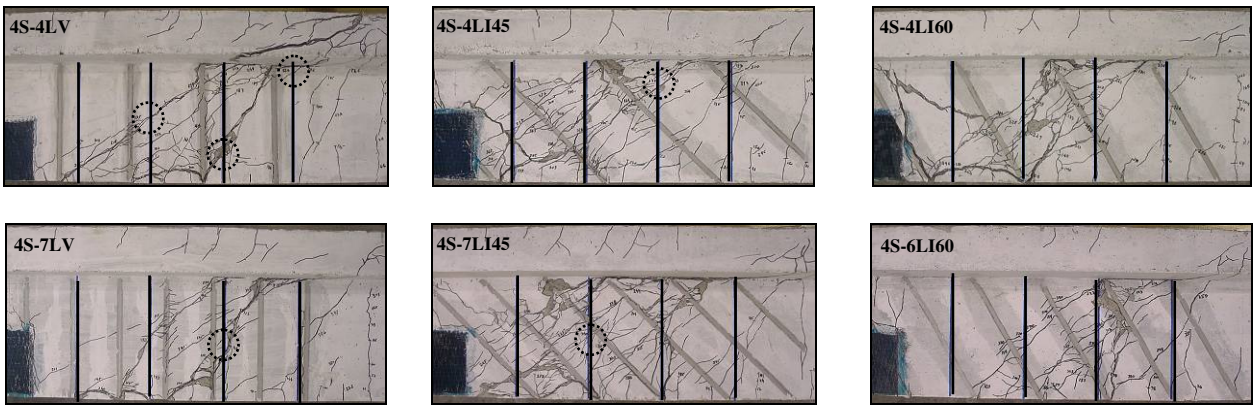

Fig. 13 - Details of the failure zones of the NSM strengthened beams with ρ_{sw} = 0.17%

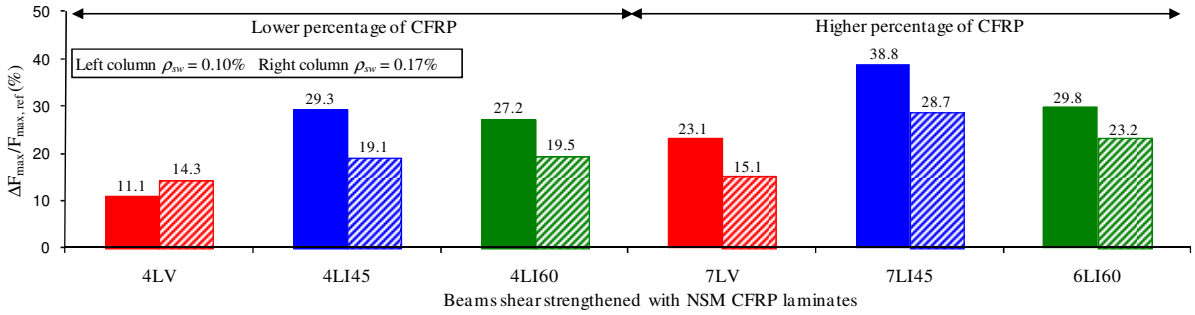

Fig. 14 - Influence of the percentage of existing steel stirrups in the effectiveness of the NSM shear strengthening technique using CFRP laminates

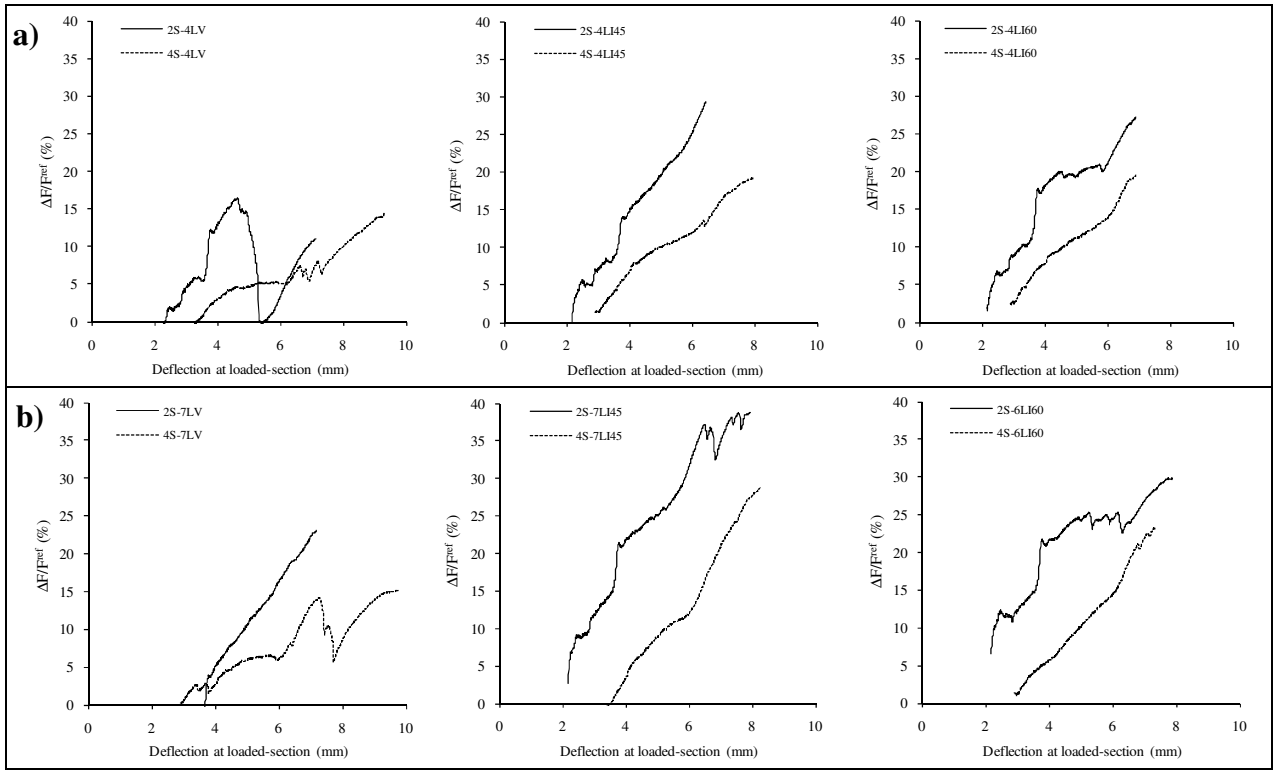

Fig. 15 - $\Delta F/F^{ref}$ *vs* deflection at the loaded-section for the beams shear strengthened with NSM CFRP laminates (beams with ρ_{sw} = 0.10%: continuous line; beams with ρ_{sw} = 0.17%: dashed line): a) lowest percentage of CFRP; b) intermediate percentage of CFRP